In-situ vehicular antenna integration and design aspects for vehicle-to-vehicle communications

Thiel, Andreas; Klemp, Oliver; Paier, Alexander; Bernadó, Laura; Kåredal, Johan; Kwoczek, Andreas

Published in:
[Host publication title missing]

2010

In-Situ Vehicular Antenna Integration and Design Aspects for Vehicle-to-Vehicle Communications

Andreas Thiel*, Oliver Klemp*, Alexander Paier†, Laura Bernadó‡, Johan Karedal§, Andreas Kwoczek¶
*Delphi Delco Electronics Europe GmbH
Bad Salzdetfurth, Germany
Contact: {andreas.thiel, oliver.klemp}@delphi.com
†Institut für Nachrichtentechnik und Hochfrequenztechnik, Technische Universität Wien
Vienna, Austria
‡Forschungszentrum Telekommunikation Wien (ftw.)
Vienna, Austria
§Department of Electrical and Information Technology, Lund University
Lund, Sweden
¶Volkswagen AG
Wolfsburg, Germany

***Abstract*—Vehicle-to-vehicle (V2V) communications aim to enhance driver safety and traffic efficiency by using the recently designated frequency bands in the $5.9\,\mathrm{GHz}$ range in Europe. Due to the time-frequency selective fading behavior of the vehicular communication channel, multi-antenna techniques can provide enhanced link conditions by means of diversity processing. This paper highlights the integration of a four-element ($N = 4$) linear array antenna into the roof-top compartment of a vehicle to conduct Multiple-Input Multiple-Output (MIMO) high-resolution mobile-to-mobile channel measurements.**

I. Introduction

Wireless V2V communication systems are currently being researched regarding their potential to reduce traffic congestion and traffic accident rates. An even higher priority of investigating the V2V radio channel in the $5\,\mathrm{GHz}$ band is caused by the recent allocation of a bandwidth of $30\,\mathrm{MHz}$ at $5.9\,\mathrm{GHz}$ which has been allocated by the European Commission in August 2008. The frequency band from $5875\,\mathrm{MHz}$ to $5905\,\mathrm{MHz}$ is especially intended for safety related intelligent transportation systems (ITS). The simulation and performance evaluation of mobile-to-mobile vehicular communication systems dramatically depends on the spatiotemporal fading behavior of the underlying propagation channels. In contrast to cellular systems, the performance in V2V communications systems is impacted by non-stationary fading conditions of the channel parameters. E. g. [1] and [2] present initial results in the $2.4\,\mathrm{GHz}$ and $5.2\,\mathrm{GHz}$ domain for V2V- and Vehicle-to-Infrastructure (V2I) channels. [3] provides an overview of recent vehicular channel measurement campaigns. Due to the presence of multiple vehicles in heavily loaded V2V communications systems and the nature of the rapidly varying channel parameters, multiple antenna techniques have gained considerable attention in the field of V2V communications. Those provide appropriate means for flexible network coverage, interference mitigation, and diversity functionality for safety-related communication applications. Based on the experience from a first V2V radio channel measurement campaign [2] in 2007, we carried out an improved multiple-input multiple-output (MIMO) V2V channel measurement campaign in the $5.6\,\mathrm{GHz}$ domain, called *DRIVEWAY*, in June 2009. The difference to the channel measurement campaign in 2007 is based on an automotive-grade realization of a MIMO antenna front-end which we now used for the mobile-to-mobile channel measurements. This paper presents an overview of the design aspects, the vehicular integration and in-situ vehicular measurements of the 4-element MIMO antenna module.

The paper is structured as follows: Sec. II describes the baseline of the underlying antenna design whereas III focuses on its vehicular integration. Sec. III-A highlights the results from an electromagnetic in-situ characterization of the antenna module on the vehicle and Sec. IV draws a conclusion.

II. Antenna Module Design Aspects

An automotive-grade antenna module including four individual antenna elements for V2V- /V2I- communications has been developed for a mobile-to-mobile channel measurement campaign *DRIVEWAY* in the specific frequency band from $5480\,\mathrm{MHz}$ to $5720\,\mathrm{MHz}$. This frequency band limitation is determined by the applied RUSK LUND channel sounder that has been used for this measurement campaign. The measurement frequencies are very close to the allocated $5.9\,\mathrm{GHz}$ frequency band for ITS in Europe and we assume the variations in the conditions of the radio channel to be negligible between $5.6\,\mathrm{GHz}$ and $5.9\,\mathrm{GHz}$.

A conventional *Volkswagen* roof-top antenna module was used as the baseline for the antenna integration. Due to the limited mounting space inside the module and especially with respect to its limited height, the antenna design was

based on a low-profile antenna prototype. With the requirement of a monopole-like radiation pattern for almost omnidirectional, terrestrial coverage, the design is based on a circular patch antenna driven in a higher operational-mode. Feeding concepts and terrestrial operational modes of the integrated patch antenna element are inline with e. g. [4]. The typical antenna layout (top-view and side-view) including an excentric feeding pin and a centered, metallic post is shown in Fig. 1. The antenna prototype is manufactured on *Rohacell* dielectric material with a sheet thickness of $t_{\mathrm{Patch}} = 1\,\mathrm{mm}$ and a relative permittivity of $\epsilon_{r,\mathrm{Patch}} \simeq 1.0$. The outer diameter of the circular patch and the shorting post amount to $d_{\mathrm{Patch}} = 10.0\,\mathrm{mm}$ and $d_{\mathrm{sp}} = 1.0\,\mathrm{mm}$. For the arrangement

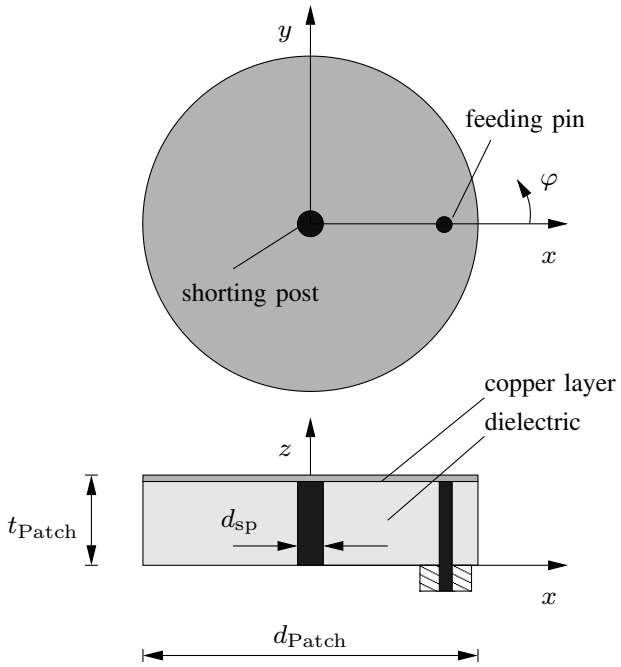

Fig. 1. Geometry of the circular patch antenna driven in a higher operational mode with feeding pin and metallic shorting post.

of the four antennas within the roof-top compound, a uniform linear array (ULA) configuration was chosen. The individual antenna elements within the ULA are separated by $\lambda/2$ at $5.6\,\mathrm{GHz}$ in order to reduce impedance-based mutual coupling effects and to compensate for a deterioration of the antenna radiation patterns, mainly in the xy-plane. Fig. 2 depicts a block diagram of the ULA including the principal location of V2V antennas within the roof-top compound. Scattering parameter measurements of the antenna module were taken when the roof-top module was mounted on a small electric ground plane (GP) featuring a diameter of $200\,\mathrm{mm}$. Impedance matching at 50Ω provides low values of the associated return loss values $S_{1,1}$ through $S_{4,4}$ for all antenna elements $\mathrm{V2V}_{\#1}$ through $\mathrm{V2V}_{\#4}$ in the order of magnitude of approx. $10\,\mathrm{dB}$ within the considered frequency band from $5.48\,\mathrm{GHz}$ to $5.72\,\mathrm{GHz}$. The respective transmission coefficients S_{21}, S_{32}, S_{43}, etc. between all four individual antenna elements range below $-12\,\mathrm{dB}$ in

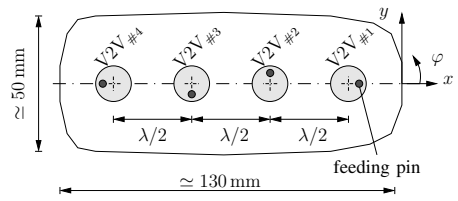

Fig. 2. Block diagram of the ULA including $N = 4$ elements $\mathrm{V2V}_{\#1}$ through $\mathrm{V2V}_{\#4}$ with feeding pins and metallic shorting posts. The $-y$-axis denotes vehicle driving direction.

the entire frequency range of operation. This is considered to be an acceptable value yielding a sufficient degree of power decoupling between all antennas.

Calibrated radiation pattern measurements of each individual V2V antenna were taken in a spherical nearfield test chamber at Delphi Delco Electronics Europe GmbH in Bad Salzdetfurth, Germany. The ULA itself and, at a later stage, the ULA integrated into the *Volkswagen* roof-top antenna module as sketched in Fig.2 were mounted on a sophisticated custom-made ground plane with diameter $d_{\mathrm{GP}} = 1\,\mathrm{m}$ and rolled edges in order to reduce diffraction effects of the electromagnetic field. The far-field antenna gain patterns of each individual antenna element are shown in Fig. 3, when the ULA is directly mounted on the GP. Tab. I presents a summary of measured vertical antenna gains including the respective angular positions $\vartheta_{\max}$ and $\varphi_{\max}$ of their observation. As can be seen from Fig. 3, each V2V antenna is characterized by an individual beam pattern coverage. This behavior is attributed by mutual coupling effects between the elements. Following Fig. 3(a) and Fig. 3(d), the relevant antenna elements $\mathrm{V2V}_{\#1}$ and $\mathrm{V2V}_{\#4}$ predominantly cover the left- and also the right halfspace centered around $\varphi = 0°$ and $\varphi = 180°$ in the azimuth plane. In contrast to this radiation behavior, the two elements $\mathrm{V2V}_{\#2}$ and $\mathrm{V2V}_{\#3}$, located in the center of the ULA point into the opposite azimuth directions of $\varphi = 90°$ and $\varphi = 270°$. The absolute $\varphi_{\max}$-positions of vertical antenna gain are given in Tab. I. As can be also seen from Tab. I, mounting the ULA on a groundplane of finite size leads to a certain beam tilt in elevation ϑ. With the circular GP, a distinct beam tilt of $\vartheta_{\max} \simeq 75°$ is observed for each individual antenna element and is attributed by a respective reduction of directive antenna gain in the xy-plane. The elements $\mathrm{V2V}_{\#1}$ and $\mathrm{V2V}_{\#2}$ are characterized by almost identical antenna gain values of $G_{\mathrm{V2V}_{\#1}} = 7.1\,\mathrm{dBil}$ and $G_{\mathrm{V2V}_{\#1}} = 7.5\,\mathrm{dBil}$. $\mathrm{V2V}_{\#3}$ and $\mathrm{V2V}_{\#4}$ exhibit lower antenna gains of $G_{\mathrm{V2V}_{\#1}} = 5.7\,\mathrm{dBil}$ and $G_{\mathrm{V2V}_{\#1}} = 4.8\,\mathrm{dBil}$.

III. Vehicular Integration

Since the *DRIVEWAY* measurement campaign focuses on the characterization of the vehicular communication channel with application-specific antenna equipment, the integration of the ULA is based on an antenna module that is ready for

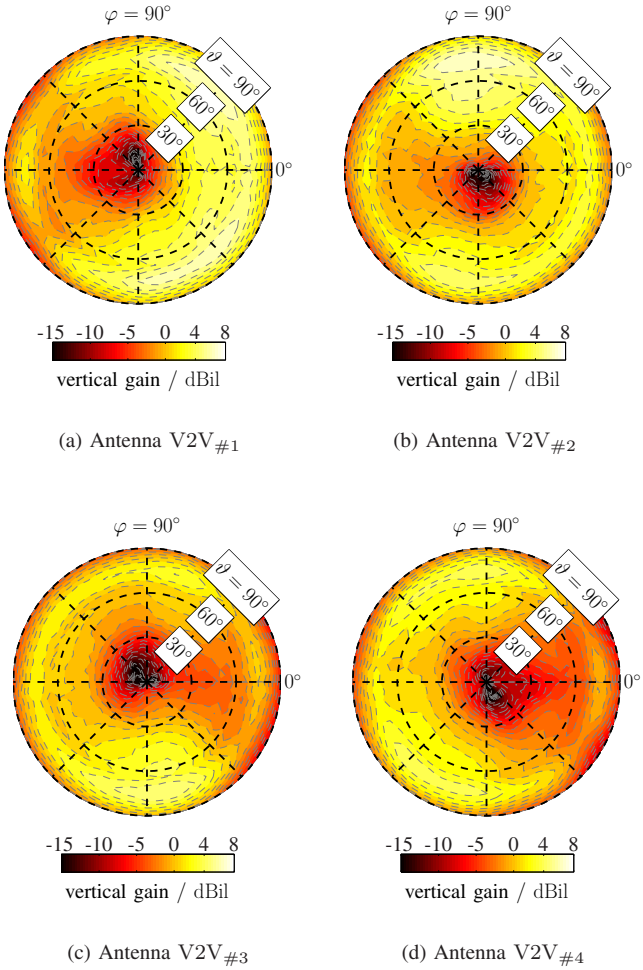

(a) Antenna $V2V_{\#1}$ (b) Antenna $V2V_{\#2}$

(c) Antenna $V2V_{\#3}$ (d) Antenna $V2V_{\#4}$

Fig. 3. ULA mounted directly on GP, calibrated far-field antenna gain pattern $V2V_{\#1}$ to $V2V_{\#4}$.

TABLE I
ANTENNA GAIN SUMMARY FOR ELEMENTS $V2V_{\#1}$ TO $V2V_{\#4}$ IF THE ULA IS DIRECTLY MOUNTED TO THE GP.

Antenna element #	G / dBil	$\vartheta_{\max}$ / °	$\varphi_{\max}$ / °
$V2V_{\#1}$	7.1	75	50
$V2V_{\#2}$	7.5	75	95
$V2V_{\#3}$	5.7	75	280
$V2V_{\#4}$	4.8	75	95

series production and which is located at a realistic mounting position on the vehicle. From the perspective of an automotive-compliant antenna integration, a relevant position for V2V antenna equipage is determined by the usual roof-top antenna module. This one is centered and -located at the back of the metallic vehicle roof. Usually, the roof-top antenna module provides functionality for a couple of different broadcasting and telecommunications services. Those typically include antennas for cellular communications, and Global Positioning System (GPS), and additional service coverage that interact with the V2V antenna front-end [5]. Fig. 4 shows the *Volkswagen Touran* measurement vehicles that were used within the *DRIVEWAY* measurement campaign. Each vehicle (one is used as a transmitter (TX), the other one is used as a receiver (RX)) is equipped as indicated with an identical antenna front-end which is installed on the conventional mounting position for roof-top antennas. Clearly, integrating the ULAs into the

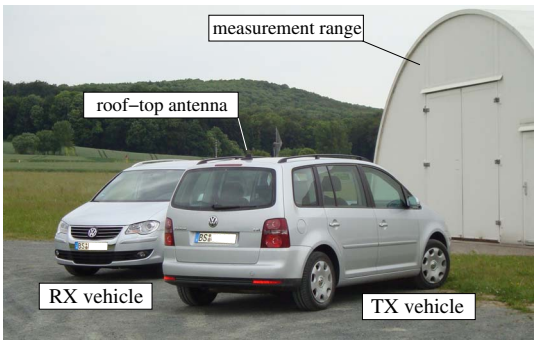

Fig. 4. TX- and RX measurement vehicles in front of the in-situ vehicular measurement facility.

roof-top antenna module causes a significant impact on the antenna radiation patterns. The applied die-cast as well as the shape of the printed circuit board and the dielectric design cover of the roof-top module lead to a significant deterioration of the related antenna far-field gain patterns. In addition to those more near-field related effects, it is also the vehicle-specific roof-top dimensions that impact on the performance of the antennas. In order to keep control of the individual degradations of the radiation behavior, $M = 6$ parasitic wire elements were integrated into the roof-top module, additionally. The geometrical length of those passive elements was chosen to be approximately $\lambda/4$ at 5.6 GHz in a way that they are able to scatter electromagnetic energy. The elements were short circuited in their respective root-points such that they act as discrete scatterers in the antenna compartment, directing electromagnetic energy into a predestined angular direction. Depending on the electrical length and distance relative to the four actively-fed antennas within the ULA, those elements can be effectively applied to achieve a distinct - but limited - degree of beam shaping. Fig. 5 depicts the location of the passive directors relative to the $N = 4$ individual antenna elements of the ULA in the xy-plane.

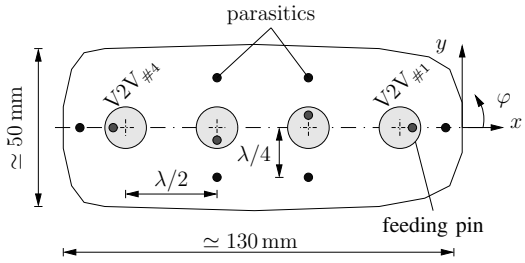

Fig. 5. Block diagram of the ULA including $M = 6$ parasitics for beam shaping.

The calibrated and measured far-field antenna gain pat-

terns for the $N = 4$ individual antennas $\mathrm{V2V}_{\#1}$ through $\mathrm{V2V}_{\#4}$ within the ULA given in Fig. 5 are shown in Fig. 6. Tab. II includes a gain summary for the ULA configuration

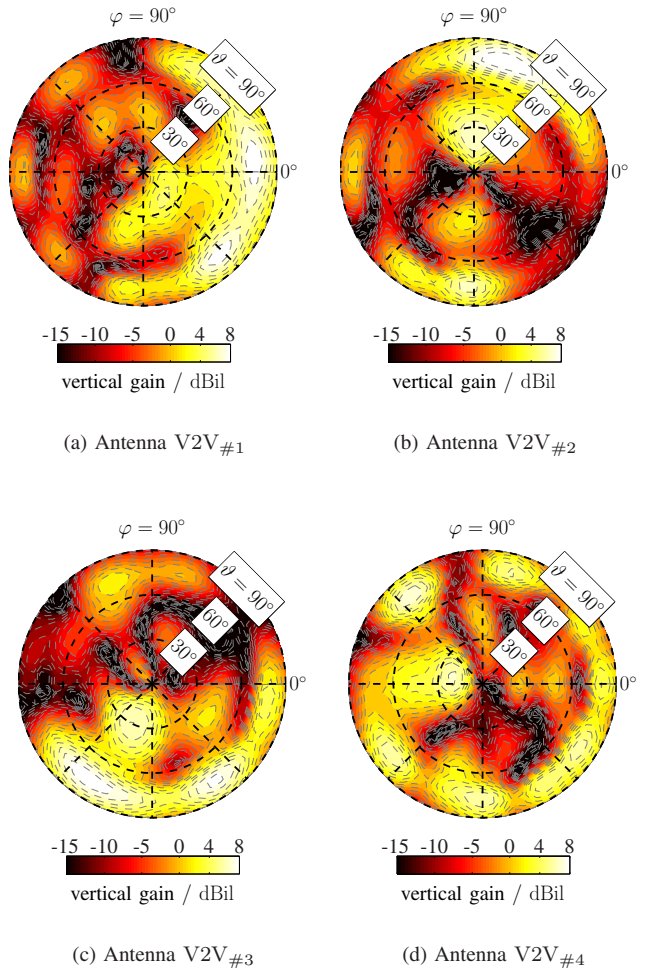

(a) Antenna $\mathrm{V2V}_{\#1}$ (b) Antenna $\mathrm{V2V}_{\#2}$

(c) Antenna $\mathrm{V2V}_{\#3}$ (d) Antenna $\mathrm{V2V}_{\#4}$

Fig. 6. ULA integrated into VW rooftop module, calibrated far-field antenna gain patterns $\mathrm{V2V}_{\#1}$ to $\mathrm{V2V}_{\#4}$.

which is embedded in the roof-top antenna module. Due to the mounting position on a rolled-edge ground plane of finite size, a distinct beam tilt towards $\vartheta_{\max} \simeq 75°$ is observed. As a consequence from the dielectric loading effects of the roof-top antenna cover, the integration of the ULA into the die-cast and the additional mounting of the aforementioned $M = 6$ parasitics, the values of antenna gain differ from the results as indicated in Tab. I for the ULA itself. $\mathrm{V2V}_{\#1}$ to $\mathrm{V2V}_{\#3}$ provide almost identical antenna gain yielding $G_{\mathrm{V2V}_{\#1}} = 9.1\,\mathrm{dBil}$, $G_{\mathrm{V2V}_{\#2}} = 9.6\,\mathrm{dBil}$ and $G_{\mathrm{V2V}_{\#3}} = 9.5\,\mathrm{dBil}$, respectively. The azimuthal positions of maximum antenna gain are observed at $\varphi_{\max,\mathrm{V2V}_{\#1}} = 5°$, $\varphi_{\max,\mathrm{V2V}_{\#2}} = 75°$ and $\varphi_{\max,\mathrm{V2V}_{\#3}} = 235°$. $\mathrm{V2V}_{\#4}$ exhibits a reduced antenna gain of $G_{\mathrm{V2V}_{\#4}} = 7.8\,\mathrm{dBil}$ which is observed at $\vartheta_{\max} = 75°$ and $\varphi_{\max} = 130°$. This gain reduction can also be derived from Fig. 6(d) that clearly indicates a more uniform gain distribution for $\mathrm{V2V}_{\#4}$ in the azimuth plane φ centered around $\vartheta_{\max} \simeq 75°$.

TABLE II
GAIN SUMMARY FOR ELEMENTS $\mathrm{V2V}_{\#1}$ TO $\mathrm{V2V}_{\#4}$ IF THE ULA IS INTEGRATED INTO THE ROOF-TOP ANTENNA MODULE.

Antenna element #	G / dBil	$\vartheta_{\max}$ / °	$\varphi_{\max}$ / °
$\mathrm{V2V}_{\#1}$	9.1	75	5
$\mathrm{V2V}_{\#2}$	9.6	75	75
$\mathrm{V2V}_{\#3}$	9.5	75	235
$\mathrm{V2V}_{\#4}$	7.8	75	130

A. Results

Following the presented measurements of the ULA located on a GP with diameter $d_{\mathrm{GP}} = 1\,\mathrm{m}$ and rolled edges as in the preceding Section II and for the modified module as in Section III , this section highlights the effects of realistic vehicular antenna integration and presents measurement results on vehicle level. This implies integrating the ULA into the automotive antenna module as depicted in Fig. 2 and mounting the module on the vehicle roof-top as shown on Fig. 4.
The ULAs as described in Sec. III are integrated into the roof-top modules and placed on the back of the roof-top of the TX- and RX car as shown in Fig. 4. The *Volkswagen* antenna housings are oriented perpendicular to driving direction in a way that the ULA is also oriented perpendicular to the driving direction. Considering the antenna positions as shown in Fig. 5, antenna element $\mathrm{V2V}_{\#1}$ is oriented to the left of the measurement vehicle and antenna element $\mathrm{V2V}_{\#4}$ is oriented to the right. Both directions are defined with respect to the driving direction of the vehicle that is assumed along the $-y$-axis as depicted in Fig. 5.
Calibrated radiation pattern measurements of the V2V antenna modules mounted on the measurement vehicles were taken in an automated 3D nearfield measurement facility at Delphi Delco Electronics Europe GmbH in Bad Salzdetfurth, Germany. The vehicle was placed on a conductive turntable (diameter $d = 6\,\mathrm{m}$) which is embedded in a circular conductive floor with $d = 24\,\mathrm{m}$ in diameter. Fig. 7 depicts the calibrated far-field antenna gain patterns of the individual elements $\mathrm{V2V}_{\#1}$ to $\mathrm{V2V}_{\#4}$. Tab. III includes a summary of antenna gains for the in-situ vehicular antenna measurements. Following the design flow as described in Sec. III, the $M = 6$ passive wire elements effectively improve the shape of the related antenna beam patterns. Element $\mathrm{V2V}_{\#1}$ which is

TABLE III
GAIN SUMMARY FOR CALIBRATED IN-SITU VEHICULAR MEASUREMENTS OF $\mathrm{V2V}_{\#1}$ THROUGH $\mathrm{V2V}_{\#4}$.

Antenna element #	G / dBil	$\vartheta_{\max}$ / °	$\varphi_{\max}$ / °
$\mathrm{V2V}_{\#1}$	7.8	75	10
$\mathrm{V2V}_{\#2}$	6.8	80	100
$\mathrm{V2V}_{\#3}$	7.5	80	280
$\mathrm{V2V}_{\#4}$	3.4	75	165

pointing at $\vartheta_{\max} = 75°$, $\varphi_{\max} = 10°$ comprises a directive gain in the order of magnitude of $G_{\mathrm{V2V}_{\#1}} = 7.8\,\mathrm{dBil}$ for the

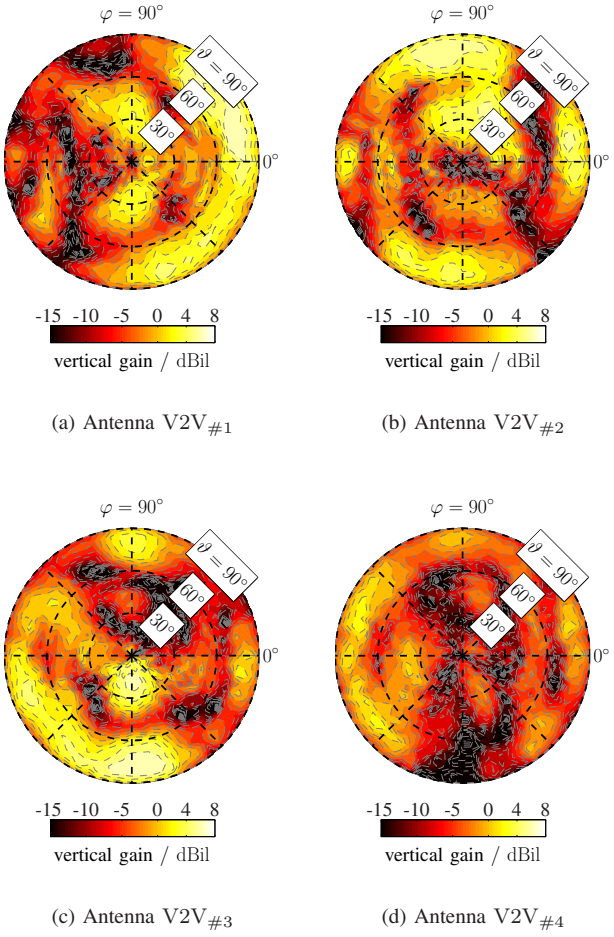

(a) Antenna $\mathrm{V2V}_{\#1}$ (b) Antenna $\mathrm{V2V}_{\#2}$

(c) Antenna $\mathrm{V2V}_{\#3}$ (d) Antenna $\mathrm{V2V}_{\#4}$

Fig. 7. In-situ vehicle measurement results, calibrated far-field antenna gain patterns $\mathrm{V2V}_{\#1}$ to $\mathrm{V2V}_{\#4}$.

vertical component of the antenna far-field. The vertical far-field gain of $\mathrm{V2V}_{\#4}$ amounts to $G_{\mathrm{V2V}_{\#4}} = 3.4\,\mathrm{dBil}$ and is observed at $\vartheta_{\max} = 75°$, $\varphi_{\max} = 165°$. The antenna elements $\mathrm{V2V}_{\#2}$ and $\mathrm{V2V}_{\#3}$ that are located close to the center of the ULA provide vertical antenna gains of $G_{\mathrm{V2V}_{\#2}} = 6.8\,\mathrm{dBil}$ and $G_{\mathrm{V2V}_{\#3}} = 7.5\,\mathrm{dBil}$. The latter two antennas are both pointing bi-directional into the half-spaces centered around $\varphi = 90°$ and $\varphi = 270°$. $\mathrm{V2V}_{\#2}$ provides its maximum gain at $\vartheta_{\max} = 80°$, $\varphi_{\max} = 100°$ whereas $\mathrm{V2V}_{\#3}$ is pointing to $\vartheta_{\max} = 80°$, $\vartheta_{\max} = 280°$. The slightly increased beam tilt of $\vartheta_{\max} = 80°$ for $\mathrm{V2V}_{\#2}$ and $\mathrm{V2V}_{\#3}$ is attributed by the distinct roof-top curvature of the measurement vehicles.

IV. Conclusion

This paper focuses on the design of an automotive-grade four-element ($N = 4$) uniform linear antenna (ULA) array which is integrated into a realistic roof-top antenna module for a high-resolution vehicle-to-vehicle measurement campaign. The antenna elements are based on the concept of a circular patch which is driven in a higher operational mode, thus leading a terrestrial radiation pattern. $M = 6$ passive and resonant metallic wire elements were integrated into the roof-top module in order to compensate for mutual-coupling based deteriorations of the antenna radiation patterns and vehicular integration effects. Calibrated radiation pattern measurements were taken for the ULA on module level in a spherical near-field test chamber as well as on the vehicle level in a vehicular in-situ measurement facility.

References

[1] G. Acosta and M. A. Ingram, "Model development for the wideband expressway vehicle-to-vehicle 2.4 GHz channel," *Proceedings of the IEEE Wireless Communications and Networking Conference*, 3-6 April 2006.

[2] A. Paier, J. Karedal, N. Czink, H. Hofstetter, C. Dumard, T. Zemen, F. Tufvesson, A. F. Molisch, and C. F. Mecklenbräuker, "Car-to-Car Radio Channel Measurements at 5 GHz: Pathloss, Power-Delay Profile, and Delay-Doppler Spectrum," *Proceedings of the 4^{th} IEEE International Symposium on Wireless Communication Systems*, vol. 1, pp. 224–228, 17-19 October 2007.

[3] A. F. Molisch, F. Tufvesson, J. Karedal, and C. F. Mecklenbräuker, "Propagation aspects of vehicle-to-vehicle communications - an overview," *Proceedings of the 2009 IEEE Radio and Wireless Symposium*, vol. 1, pp. 179–182, 18-20 January 2009.

[4] V. González-Posadas, D. Segovia-Vargas, E. Rajo-Iglesias, J. L. Vázquez-Roy, and C. Martín-Pascual, "Approximate Analysis of Short Circuited Ring Patch Antenna Working at TM_{01} Mode," *IEEE Transactions on Antennas and Propagation*, vol. 54, no. 6, pp. 1875–1879, 2006.

[5] A. Thiel and O. Klemp, "Initial Results of Multielement Antenna Performance in 5.85GHz Vehicle-to-Vehicle Scenarios," *Proceedings of the 2008 European Conference on Wireless Technology, Amsterdam, The Netherlands, 2008*, vol. 1, pp. 322–325, 2008.